Hardening measures for bipolar transistors against microwave-induced damage*

Chai Chang-Chun(柴常春), Ma Zhen-Yang(马振洋)†, Ren Xing-Rong(任兴荣), Yang Yin-Tang(杨银堂), Zhao Ying-Bo(赵颖博), and Yu Xin-Hai(于新海)

School of Microelectronics, Key Laboratory of Ministry of Education for Wide Band-Gap Semiconductor Materials and Devices, Xidian University, Xi'an 710071, *China*

(Received 23 September 2012; revised manuscript received 30 November 2012)

In the present paper we study the influences of the bias voltage and the external components on the damage progress of a bipolar transistor induced by high-power microwaves. The mechanism is presented by analyzing the variation in the internal distribution of the temperature in the device. The findings show that the device becomes less vulnerable to damage with an increase in bias voltage. Both the series diode at the base and the relatively low series resistance at the emitter, R_e, can obviously prolong the burnout time of the device. However, R_e will aid damage to the device when the value is sufficiently high due to the fact that the highest hot spot shifts from the base-emitter junction to the base region. Moreover, the series resistance at the base R_b will weaken the capability of the device to withstand microwave damage.

Keywords: bipolar transistor, high-power microwave, hardening measures

PACS: 85.30.Pq, 84.40.–x **DOI:** 10.1088/1674-1056/22/6/068502

1. Introduction

High-power microwaves (HPMs) pose a serious threat to electronic systems. Different HPM sources may cause a disruption or destruction of the semiconductor components of the system.[1–10] At the same time, the higher safety and stability demands of electronic systems require further development of the protection measures against electromagnetic interference. The need for suitable hardening measures has emerged during the past several years, and some attempts have been made to protect the system from these effects. An electromagnetic topological approach was utilized to develop a consistent shielding protection method to protect complex electronic systems from electromagnetic environments.[11] Brauer *et al*.[12] investigated the different hardening measures for susceptible coupling paths of an IT system under different high-power electromagnetic conditions. The results indicated that enhanced line filters and the subdivision of enclosures can be applied to systems to protect them from electromagnetic interference. The vulnerability and the mitigation measurement of future electrified railway systems in Europe from a HPM source were investigated.[9] Surge protection devices, such as gas discharge tubes and metal–oxide varistors, are not suitable for protection against HPM and ultra-wideband (UWB) pulses due to their slow activation time, while diode limiters can better protect the system against HPM and UWB pulses, but lead to an additional 7-dB increase in the power level for permanent damage. All the hardening investigations indicate that the study of efficient protection measures for electronic systems is one of the profound tasks. However, the hardening measures for device failure levels are particularly lacking, so device level hardening measures and effect studies are required in order to better understand the effect of these electronic systems and the interference mechanism.

In our previous studies we established a two-dimensional (2D) electro–thermal model of a typical bipolar transistor and studied the damage effect and mechanism of the device, caused by microwaves, and the effects of some important parameters such as pulse width and frequency on the damage process.[13–16] In the present paper, the hardening measures for the bipolar transistor against the microwaves are studied theoretically. The influences of the bias voltage and the external components such as the diode and the series resistances on the device damage process induced by microwaves are also investigated. Meanwhile, the internal mechanism is presented utilizing the 2D electro–thermal model. It is demonstrated that the bias voltage and the external components can change the speed of the device damage.

2. Device structure

Figure 1 shows a schematic diagram of the analyzed silicon n^+–p–n–n^+ epitaxial planar transistor used in our calculation, and only half of the central emitter finger is analyzed, owing to the geometrical symmetry. The bulk of the transistor is a 200 μm-thick n^+-type collector substrate, above which is a 2 μm-thick n-type epitaxial layer. The device thickness along the z axis is 1 μm. The collector metallization is shown below the substrate. B, C, and E denote its base, collector, and emitter contacts, respectively. N^+ denotes the heavily doped region of

*Project supported by the National Natural Science Foundation of China (Grant No. 60776034).

†Corresponding author. E-mail: zyma@mail.xidian.edu.cn

© 2013 Chinese Physical Society and IOP Publishing Ltd

the n-type silicon, and P refers to the p-type base region. The doping profile of the typical bipolar junction transistor (BJT) is given in Fig. 2. The thermal electrode is specified at the bottom of the transistor, where the lattice temperature is assumed to be a constant ($T_0 = 300$ K). The upper surface (along line $y = 0$ μm) and the sidewall boundaries (along line $x = 0$ μm and $x = 10$ μm) are thermally insulated from the environment, so we have

$$\partial T/\partial y\big|_{y=0} = 0, \tag{1}$$

$$\partial T/\partial x\big|_{x=0,10} = 0. \tag{2}$$

The frequency of the injected signals selected in our simulation is 1 GHz, which is of most interest for the HPM effects.[17] The continuous sinusoidal voltage with a frequency of 1 GHz is injected from the collector contact. By using the 2D device simulator ISE-TCAD, the authors take the device lattice temperature reaching the silicon melting point of 1688 K as the burnout criterion.

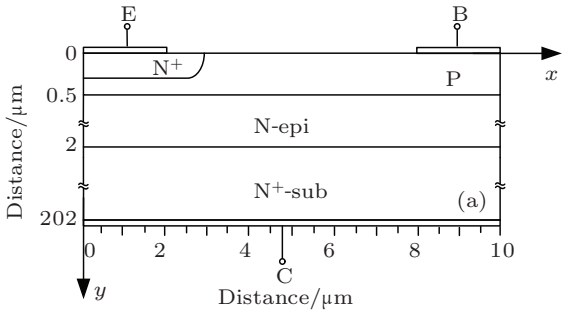


Fig. 1. The device structure of an n^+–p–n–n^+ transistor.

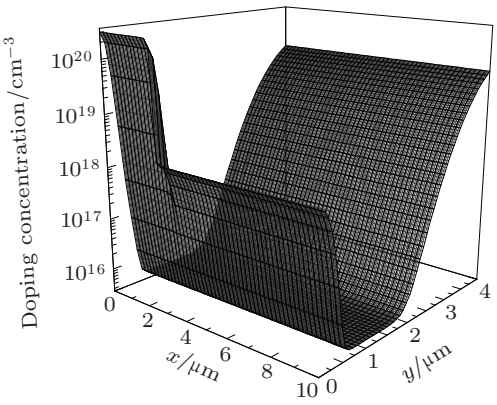


Fig. 2. The doping profile of the BJT.

3. Results and analysis

3.1. The influence of the bias voltage on the damage process

The simulation circuit is shown in Fig. 3, in which the transistor is in the active mode of operation. By changing the external resistances, we can control the bias voltage V_{CE} precisely. The bias voltage is increased from 1 V to 11 V, while the injected signals remain the same. Figure 4 illustrates the dependences of the burnout time and the bias voltage on the condition that the injected voltage magnitudes are $U_0 = 45$ V and $U_0 = 50$ V, respectively. The figure shows that the burnout time increases linearly with increasing bias voltage. For the $U_0 = 45$ V and $U_0 = 50$ V cases, their burnout times at $V_{CE} = 11$ V are almost twice their corresponding values at $V_{CE} = 1$ V. Therefore, we conclude that the device becomes less vulnerable to damage as the bias voltage increases.

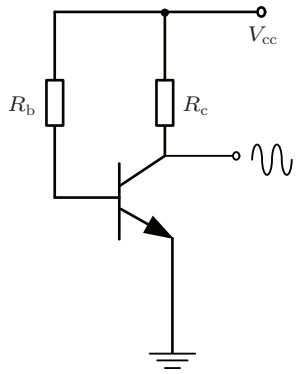


Fig. 3. Schematic diagram of the circuit used in our simulation.

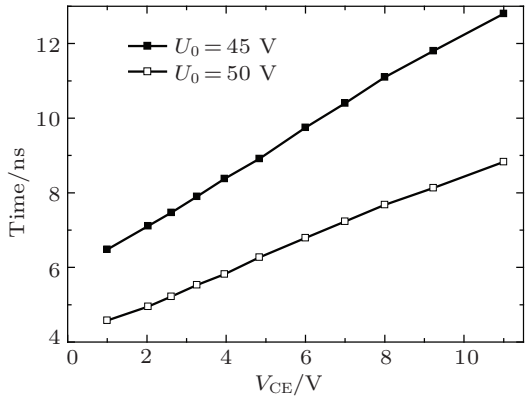


Fig. 4. The dependences of the burnout time on V_{CE} for the cases of $U_0 = 45$ V and 50 V.

In the previous paper we presented the damage effect and the mechanism of a bipolar transistor, caused by microwaves, which showed that the base-emitter junction was susceptible to damage, and that the thermal accumulation occurred mostly in the negative half-period.[13,14] In the operation state of the bipolar transistor, the base-emitter junction is forward biased and the base-collector junction is reversely biased. The voltage drop is mainly across the base-collector junction. In the negative half-period of the injected signal, when the absolute value of the injected voltage is larger than the value of V_{CE}, the base-emitter junction is reversely biased and the base-collector is forward biased.[13] Due to the fact that the emitter-base junction has a low breakdown voltage, the high current density and the high reverse electric field lead to a certain heat quantity.

The higher the value of V_{CE}, the lower the reverse-biased voltage is and the less the dissipated power is across the base-emitter junction. Therefore, the burnout time will increase with the value of V_{CE} increasing. Meanwhile, as the amplitude of the injected voltage increases, the reverse biased voltage across the base-emitter junction also increases and the burnout time decreases, which is also depicted in Fig. 4. However, the increase in the bias voltage will lead to excessive power consumption, so we should make a tradeoff between the two factors.

3.2. The influence of the external diode at the base

The simulation circuit with an external diode at the base is illustrated in Fig. 5, in which the transistor is in the active mode of operation. Some of the diode model parameters used in our simulation are shown in Table 1.[18] In the operating state of the transistor, the reverse-biased diode has a high resistance and the circuit between the base and the ground is under open-circuit condition. The reverse breakdown voltage of the diode is much higher than the voltage across the base-emitter junction. Even if the breakdown occurs in the diode, the current at the reverse breakdown voltage is designed to be a low value so that it has little influence on the performance of the circuit. Figure 6 shows the influence of the external diode at the base on the burnout time. It indicates that the burnout time decreases as the amplitude of the injected signal increases, and the burnout time of the device with the external diode at the base is longer than that without the external diode under the same magnitude of injected voltage.

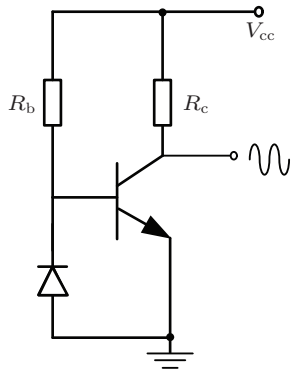


Fig. 5. Schematic diagram with the external diode at the base.

Table 1. Some important diode model parameters in our simulation.[18]

Diode model parameter	Value	Unit
Saturation current	0.1	pA
Ohmic resistance	16	Ω
Junction capacitance	2	pF
Transit time	12	ns
Reverse breakdown voltage	100	V
Current at the reverse breakdown voltage	0.1	pA

In the negative half-period of the injected signal, both the base-collector junction and the external diode at the base are forward-biased on the condition that the absolute value of the injected voltage exceeds the sum of the two forward turn-on voltages of the external diode and the base-collector junction. Therefore, a conductive pathway forms between the collector and the ground, and most of the current injected from the collector will flow to the ground through it. The base-emitter junction will not break down easily compared with the condition without the external diode at the base. So the accumulated heat will decrease and the burnout time will increase simultaneously.

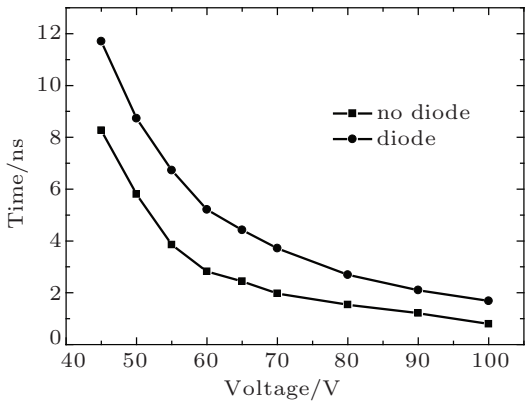


Fig. 6. Dependences of burnout time on injected voltage in the case without and with an external diode.

3.3. The influence of the external resistor R_e at the emitter

In the present paper, the influence of an emitter series resistance of 40 Ω on the microwave damage process is studied. The results show that the capability of the device to withstand microwave damage is enhanced effectively. In this subsection, the series resistances varies from 1 Ω to 400 Ω and the simulation circuit is shown in Fig. 7, in which the emitter and the base are connected to the ground. The dependence of the peak temperature at the end of the first 10 cycles on the series resistance at the emitter is depicted in Fig. 8. It shows that there is an inflexion point at around 50 Ω. The peak temperature decreases linearly with series resistance increasing when the series resistance is smaller than 50 Ω, but increases rapidly when the series resistance is larger than the inflexion point. The peak temperature with $R_e = 400$ Ω is 100 K higher than that with $R_e = 5$ Ω.

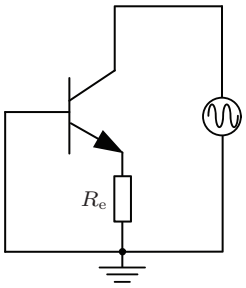


Fig. 7. Schematic diagram with the external resistor R_e at the emitter.

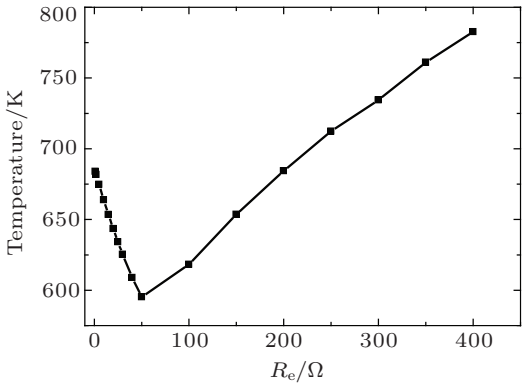


Fig. 8. Dependence of the peak temperature after the first 10 cycles on R_e.

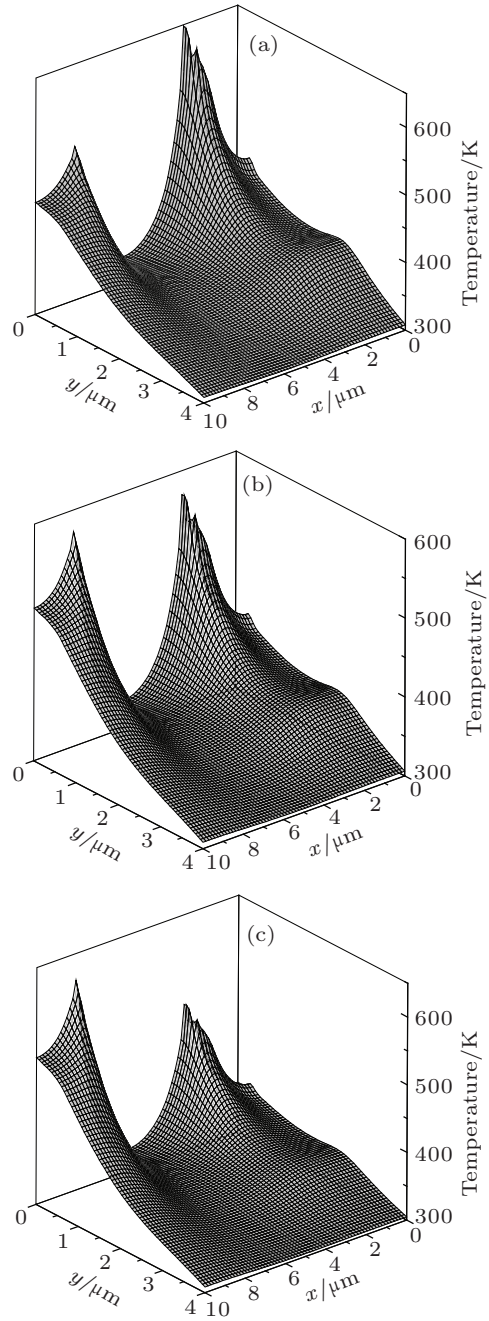


Fig. 9. Temperature distributions of the device after the first 10 cycles for different emitter series resistances: (a) $R_e = 5\ \Omega$; (b) $R_e = 50\ \Omega$; (c) $R_e = 100\ \Omega$.

Figure 9 depicts the temperature distributions of the device at the end of the first 10 cycles for different series resistances. In the absence of the series resistance, the temperature-rising position is located on the edge of the emitter region near the base. When the series resistance is relatively low, the hot spot in the base region cannot be neglected (Fig. 9(a)). In the negative half-period, the voltage drop occurs across the emitter series resistance due to the large current density generated in the emitter region. A negative feedback effect will lead to a decrease in the voltage drop across the emitter region, and the emitter current density will fall at the same time. Therefore, the peak temperature there decreases naturally. Meanwhile, the base current density will increase under the condition of the same injected voltage, and the dissipated power in the base region will increase. The higher the emitter series resistance, the lower the emitter current density is and the higher the base current density is. In a word, the peak temperature in the base region increases with increasing emitter series resistance. When the emitter series resistance increases to 50 Ω, the peak temperature in the emitter region is almost the same as in the base region (Fig. 9(b)). The highest temperature position shifts from the base-emitter junction to the base region as the emitter series resistance continues to increase (Fig. 9(c)). It is illustrated that the exorbitant series resistance will not enhance the capability of the transistor to withstand microwave signals, but aggravates the device damage process. It is suggested that a series resistance lower than 50 Ω is appropriate for the device used in our simulation.

3.4. The influence of the external resistor R_b at the base

The simulation circuit with an external resistance R_b at the base is illustrated in Fig. 10. The bipolar transistor is injected by a signal from the collector, with the amplitude setting at 30 V. The base series resistance is swept over 1 Ω to 400 Ω. Figure 11 depicts the relationship between the peak temperature at the end of the tenth cycle and the base series resistance. It shows that the peak temperature increases obviously with increasing base series resistance. The peak temperature in the $R_b = 400\ \Omega$ case is about 890 K, which is increased by 200 K compared with the value in the $R_b = 1\ \Omega$ case. In other words, the burnout time will decrease with increasing base series resistance.

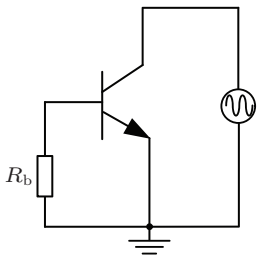


Fig. 10. Schematic diagram with the external resistor R_b at the emitter.

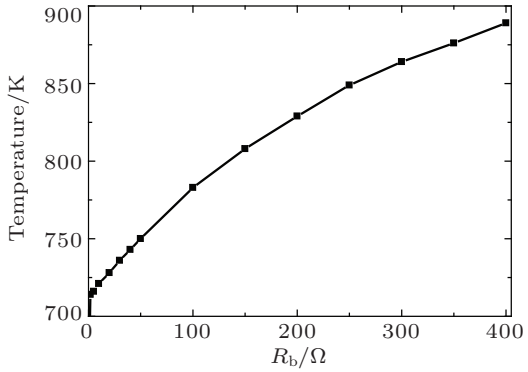


Fig. 11. The dependence of the peak temperature after the first 10 cycles on R_b.

Figure 12 depicts the distributions of temperature along the line $y = 0.1$ μm after the first 10 cycles with different base series resistances. It is illustrated that the temperature in the emitter region increases as the base series resistance increases from 25 Ω to 300 Ω. Meanwhile, the temperature in the base region decreases with increasing base series resistance. In the negative half-period of the injected signal, the base-collector junction is forward-biased when the absolute value of the injected voltage exceeds the forward turn-on voltage of the base-collector junction, and the resistance between the base electrode and the collector electrode is mainly composed of the base resistance and the collector resistance. For a certain amplitude of the injected voltage, the voltage drop across the base series resistance increases with the increasing base series resistance, and the absolute value of the reverse voltage between the emitter electrode and the base electrode increases. Therefore, the breakdown of the base-emitter junction occurs more easily, and the temperature rise in the emitter region will increase with increasing base series resistance. Furthermore, the joule heat in the base region is mainly determined by the current density due to the relatively low electric field in the base region. The base current density decreases with increasing base series resistance, and the joule heat in the base region decreases at the same time.

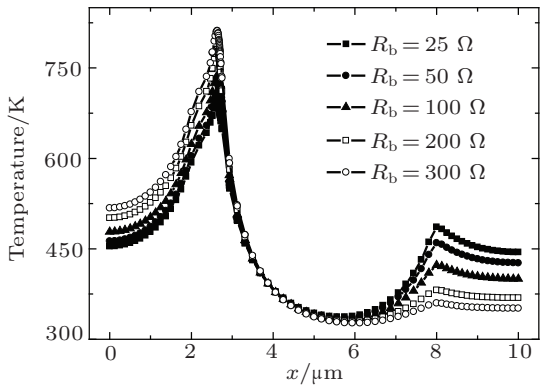


Fig. 12. The distributions of temperature across the B–E junction after the first 10 cycles for different values of R_b (along the line $y = 0.1$ μm).

4. Conclusion

In this paper, measures are developed to improve the protection of a typical bipolar transistor against microwave-induced damage. The investigation indicates that appropriate external components can improve the protection of the device against microwave interference. The increasing bias voltage will lengthen the burnout time of the device, which implies that microwave interference effects on next-generation integrated circuits will become more dominant, since the bias voltage drops in proportion to the minimum technology size. This factor increases the demand for future investigations on the hardening measures. We also studied the influence of external components such as the series resistance and the diode on the device damage process. The series diode at the base will discharge the injected current when the absolute value of the injected voltage is high enough, and a relatively low R_e will slow the rise of the peak temperature of the device, both of which will effectively protect a typical bipolar transistor against microwave damage. However, the series resistance R_b at the base and a higher R_e show no improvement for device protection against microwave interference.

References

[1] Palisek L and Suchy L 2011 *Proceedings of EMC Europe* 2011 *York — 10th International Symposium on Electromagnetic Compatibility*, September 26–30, 2011 York, United Kingdom, p. 18
[2] Ren Z, Yin W Y, Shi Y B and Liu Q H 2010 *IEEE Trans. Electron. Dev.* **57** 345
[3] Kim K and Iliadis A A 2010 *Solid-State Electron.* **54** 18
[4] Iliadis A A and Kyechong K 2010 *IEEE Trans. Dev. Mater. Reliab.* **10** 347
[5] Wang H Y, Li J Y, Zhou Y H, Hu B and Yu X Y 2009 *Electromagnetics* **29** 393
[6] Kanyou Nana R, Korte S, Dickmann S, Garbe H and Sabath F 2009 *Adv. Radio Sci.* **7** 249
[7] Wang H, Li J, Li H, Xiao K and Chen H 2008 *Prog. Electromagn. Res.* **87** 313
[8] Mansson D, Thottappillil R, Nilsson T, Lunden O and Backstrom M 2008 *IEEE Trans. Electromagn. Compat.* **50** 434
[9] Mansson D, Hottappillil R, Backstrom M and Lunden O 2008 *IEEE Trans. Electromagn. Compat.* **50** 101
[10] Chai C C, Xi X W, Ren X R, Yang Y T and Ma Z Y 2010 *Acta Phys. Sin.* **59** 8118 (in Chinese)
[11] Baker G, Castillo J P and Vance E F 1992 *IEEE Trans. Electromagn. Compat.* **34** 267
[12] Brauer F, Fahlbusch S, Haseborg J L and Potthast S 2012 *IEEE Trans. Electromagn. Compat.* **54** 1055
[13] Ma Z Y, Chai C C, Ren X R, Yang Y T and Chen B 2012 *Acta Phys. Sin.* **61** 078501 (in Chinese)
[14] Ma Z Y, Chai C C, Ren X R, Yang Y T, Chen B and Zhao Y B 2012 *Chin. Phys. B* **21** 058502
[15] Ma Z Y, Chai C C, Ren X R, Yang Y T, Chen B, Song K and Zhao Y B 2012 *Chin. Phys. B* **21** 098502
[16] Ma Z Y, Chai C C, Ren X R, Yang Y T, Zhao Y B and Qiao L P 2013 *Chin. Phys. B* **22** 028502
[17] Radasky W A 2010 *Asia-Pacific Symposium on Electromagnetic Compatibility*, April 12–16, Beijing, China, p. 758
[18] Integrated Systems Engineering Corp. 2004 *ISE-TCAD Dessis Simulation User's Manual*, Zurich, Switzerland, 2004 p. 208